Monitoring Plant Health Using Multispectral Satellite Imagery Based on Various Spectral Indices

Samanta, S.
School of Surveying and Land Studies, The Papua New Guinea University of Technology, Lae, Morobe, Papua New Guinea, E-mail: rsgis.sailesh@gmail.com
DOI: https://doi.org/10.52939/ijg.v21i11.4593

Abstract
Multispectral satellite images acquired through remote sensing can identify, estimate, monitor, and manage the ecological environment, agricultural health, drought, and yield. This paper compares the effectiveness of the Temperature Vegetation Dryness Index (TVDI) and Vegetation Health Index (VHI) in plant growth monitoring. An oil palm plantation owned by New Britain Palm Oil Limited (NBPOL) near Erap station, within the Markham River basin, was selected for this study. Multispectral bands, like red, near-infrared, shortwave infrared, and thermal bands of a Landsat 8 Satellite, were utilized to produce land surface temperature (LST) and normalized difference vegetation index (NDVI) databases, which are key parameters for calculating the Vegetation Condition Index (VCI) and Temperature Condition Index (TCI). These VCI and TCI indices were then used in the VHI and TVDI models. The VHI ranged from 11.83 to 87.78, while the TVDI ranged from 0.142 to 0.969. Low VHI values and high TVDI values indicate extreme drought conditions. A strong coefficient of determination was found between LST and VHI (R^2 = 0.89) and between NDVI and VHI (R^2 = 0.88), indicating that NDVI and LST are equally crucial for assessing vegetation health. Conversely, a near-perfect correlation was observed between LST and TVDI (R^2 = 0.98), compared to NDVI and TVDI (R^2 = 0.48). The results showed that VHI offers more efficient and spatially detailed results than TVDI. The study revealed that VHI helps monitor agricultural drought by better combining vegetation condition and temperature information than other models. Furthermore, the normalized difference moisture index (NDMI) and NDVI were derived using Sentinel-2 data over 2 years. The correlation shows that the vegetation index decreases as moisture levels decline.

Keywords: Agricultural Drought, Correlation, Moisture Index, Remote Sensing, Surface Temperature, Vegetation Health, Vegetation Index

1. Introduction

Modern humans began interacting with the landscape and affecting natural ecosystems around 10 to 12 thousand years ago, transitioning from a hunting-based lifestyle to one dependent on agriculture due to initial population growth [1]. This shift is known as the first agricultural revolution. The Second Agricultural Revolution started in the 17th century and extended into the 19th century, driven by the Industrial Revolution, when human and animal labor started being replaced by machines. The world's population doubled in just 37 years, rising from approximately 2.5 billion in 1950 to 5 billion in 1987. The green revolution, or third agricultural revolution, began around 1965, utilizing modern technologies, fertilizers, pesticides, high-yielding seeds, and irrigation systems to enhance food security and address the global hunger index [2]. The land use pattern in Papua New Guinea has changed significantly due to population growth, economic development, land tenure policies, land access, and improved transportation. This change is not limited to converting natural land cover to agricultural land use. The agricultural land use pattern also changes drastically due to the introduction of new crops, the adaptation of new grains as staple foods, and increased global demand for food products and biofuels. The Markham is projected to be considered Papua New Guinea's food basket through agricultural transformation. The nation is taking the initiative through the Markham-Ramu agricultural growth corridor with the help of the International Finance Corporation. The agricultural boost in this area is planned through improving market accessibility, infrastructure development, economic growth, and enhancing national food security [3].

Ramu Agri Industries Limited (RAIL), a subsidiary of New Britain Palm Oil Limited (NBPOL), is involved in agricultural operations, such as operating the oil palm plantation, producing sugarcane, and farming cattle in the Ramu and Markham valleys. In 2008, NBPOL started converting the field used for sugarcane and other unfertile land into an oil palm plantation. Drought is the main problem for agricultural development in the Markham Valley. In 2010, 2015, and 2016, the oil palm plantation was heavily impacted by drought caused by El Niño. The normal photosynthesis process and the moisture content within the plants were affected, causing premature aging due to drought.

Over a prolonged period, little or no precipitation combined with high temperatures causes changes in soil moisture content [4]. A soil moisture deficiency is known as drought compared to its normal level [5]. Crop yields in areas without irrigation are mainly impacted by irregular rainfall, which results in higher surface temperatures and reduced yields [6]. Vegetation drought leads to significant annual losses in the Asia-Pacific region [7]. Rapid human activities and global warming also increase meteorological droughts, including their intensity, duration, and frequency [8]. Agricultural droughts were traditionally monitored using drought indicators based on in situ measurements [9]. Traditional methods for evaluating meteorological drought rely on imprecise and inaccurate station data [10] and [11]. These models have never considered variables like heat stress on vegetation growth, land use types, land cover, moisture conditions, etc. Therefore, there is a need to develop real-time, machine learning, and artificial intelligence (AI)-based drought monitoring systems instead of traditional indices to improve drought assessment, monitoring, and forecasting. The results could provide a reliable and effective method for predicting droughts and enhancing drought assessment and mitigation [12]. Critical drought-related factors can now be observed and estimated on a broader spatial and temporal scale thanks to the widespread use of remote sensing [13]. Researchers have assessed drought conditions using satellite remote sensing data and various comprehensive monitoring markers. Some of the indicators include the optimized meteorological drought index (OMDI) [14], the temperature condition index (TCI) [15], the precipitation condition index (PCI) [16], soil moisture condition index (SMI) [17], temperature vegetation dryness index (TVDI) [18] and [19], vegetation condition index (VCI) [20], and vegetation health index (VHI) [15] and [21]. TVDI is a more effective and efficient approach than other indicators because it combines the spatial distribution of vegetation characteristics with land surface temperature [22].

This study offers a practical method for monitoring plant health with multispectral satellite imagery based on various spectral indices. The main aim was to track the spatial variation of plant health using multispectral satellite imagery. The study was conducted with five objectives: (i) to analyze the spatial variation of the TVDI of the plantation area based on satellite-data-driven LST and NDVI, (ii) to perform pixel-by-pixel TCI and VCI analysis based on the previously calculated LST and NDVI, (iii) to assess and monitor plantation health spatially using the VHI, (iv) to compare drought patterns based on the resulting TVDI and VHI, and finally (v) to derive the correlation between the moisture and the vegetation index of the plantation area.

2. Study Area

A site within the Markham valley region, mainly in Morobe Province of Papua New Guinea (PNG), has been chosen as the study area. The Markham Valley region is famous for its agricultural industry, mainly palm oil plantations. The region is moderately suitable, with stony and shallow soils. The area typically experiences warm, humid conditions with an average annual rainfall of nearly 2500 mm and a mean temperature of 29°C. Rainfall occurs from December through April, with dry weather from May to December. The Erap Oil palm plantation within the Markham Valley region under Morobe province of Papua New Guinea was selected as the study site. The study area encompasses approximately 3,195 hectares, or 32 square kilometers of land within the Markham Watershed. The average age of the oil palm plantation in the site is 8 years. NBPOL and the Markham Farming Company Limited are the major investors in this oil palm plantation. The Erap River bounds the study site to the east and the Markham River to the south (Figure 1).

3. Data Used

Landsat-8 and Sentinel-2 satellite images were used to understand the health of the plantation in the spatial dimension. The standard false colour combination (SFCC) of Landsat 8 Operational Land Imager (OLI) is Band5: Band4: Band3 to Red: Green: Blue channel, whereas the SFCC of Sentinel-2 is Band8: Band4: Band3 to Red: Green: Blue channel. SFCC is extensively used for vegetation analysis, as the band combination allows healthy vegetation to look bright red.

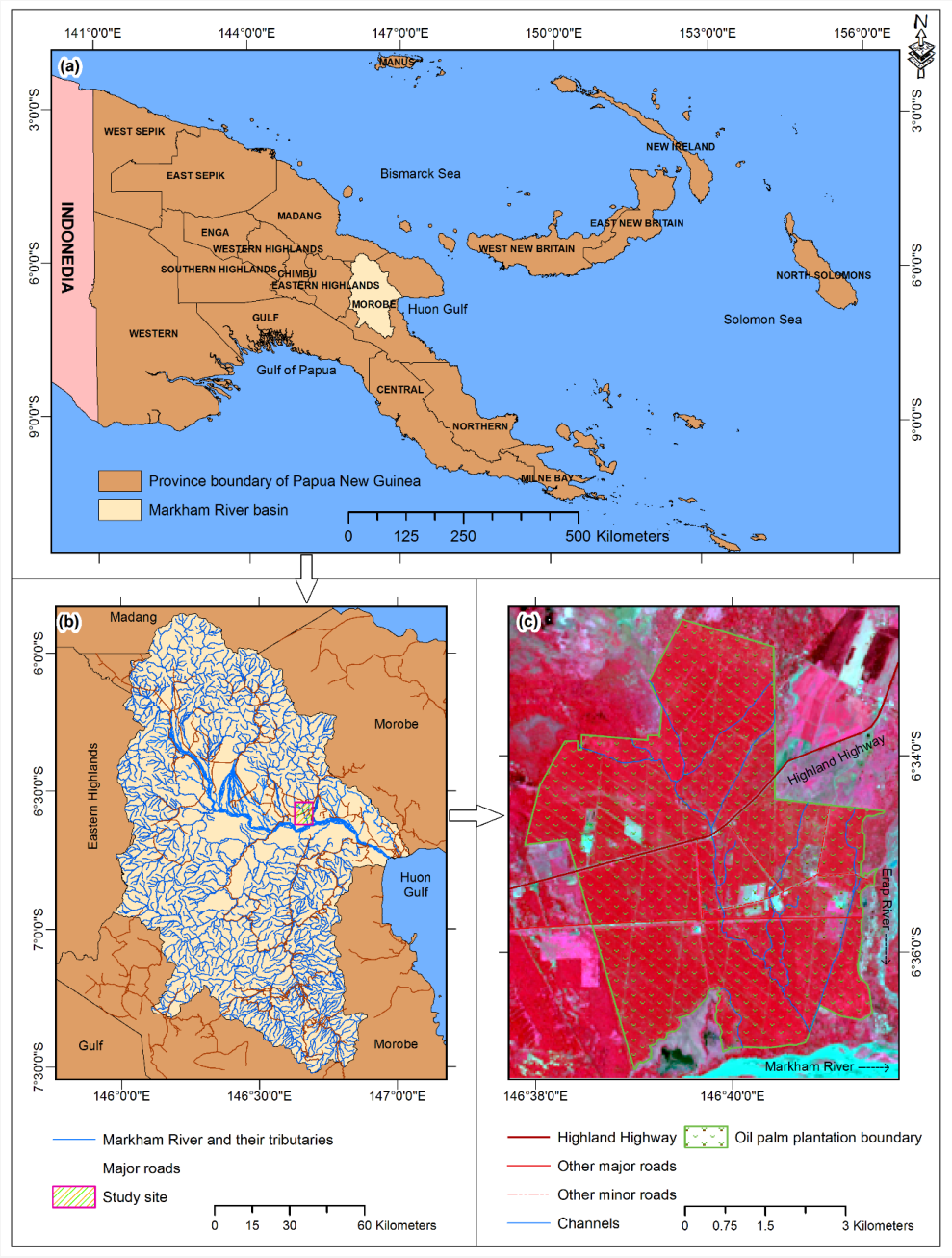

Figure 1: The locality map of the oil palm plantation (a) Provinces of Papua New Guinea with Markham River basin, (b) The Markham River basin with the highlights of the study site location, and (c) the standard false color view of the study site – NBPOL

The SFCC was used to interpret the satellite images visually. The red, near-infrared, short-wave infrared, and thermal band-1 of Landsat 8 was downloaded from Earth Explorer and used as input parameters for various spectral analyses in the spatial dimension. In contrast, multiple Sentinel-2 images were acquired from the Copernicus data space ecosystem over two years. The Sentinel-2 satellite has no thermal bands, so it was not used for TVDI and VHI analysis. Instead, these data sets were used to analyse the temporal relationship between moisture index and vegetation index over two years. Details of the Spatial and spectral band specifications of Landsat-8 and Sentinel-2 are presented in Tables 1 and 2, respectively.

Table 1: Spatial and spectral band specification of Landsat-8 Operational Land Imager (OLI) and Thermal Infrared Sensor (TIRS)

Sl. No.	Band number	Band name	Spectral range (µm)	Spatial resolution (m)
1	Band 1	Coastal aerosol	0.43 – 0.45	30
2	Band 2	Blue	0.45 – 0.51	30
3	Band 3	Green	0.53 – 0.59	30
4	Band 4	Red	0.64 – 0.67	30
5	Band 5	Near-Infrared	0.85 – 0.88	30
6	Band 6	Shortwave infrared 1	1.57 – 1.65	30
7	Band 7	Shortwave infrared 2	2.11 – 2.29	30
8	Band 8	Panchromatic (PAN)	0.50 – 0.68	15
9	Band 9	Cirrus	1.36 – 1.38	30
10	Band 10	Thermal Infrared 1	10.6 – 11.19	100
11	Band 11	Thermal Infrared 2	11.50 – 12.51	100

Table 2: Multi-spectral band specification of Sentinel-2

Sl. No.	Band number	Band name	Spectral range (µm)	Spatial resolution (m)
1	Band 1	Coastal aerosol	0.433 – 0.453	60
2	Band 2	Blue	0.458 – 0.523	10
3	Band 3	Green	0.543 – 0.578	10
4	Band 4	Red	0.650 – 0.680	10
5	Band 5	Vegetation Red Edge - 1	0.698 – 0.713	20
6	Band 6	Vegetation Red Edge -2	0.733 – 0.748	20
7	Band 7	Vegetation Red Edge - 3	0.773 – 0.793	20
8	Band 8	Near-infrared	0.785 – 0.900	10
9	Band 8A	Vegetation Red Edge - 3	0.855 – 0.875	20
10	Band 9	Water vapour	0.935 – 0.955	60
11	Band 10	Shortwave infrared - Cirrus	1.360 – 1.390	60
12	Band 11	Shortwave infrared	1.565 – 1.655	20
13	Band 12	Shortwave infrared	2.100 – 2.280	20

4. Methodology

Remote sensing has emerged as a crucial technology for analyzing and monitoring the health and growth across multiple spatial scales. USGS Earth Explorer and Copernicus have provided worldwide satellite data (Landsat, Sentinel) freely since their archive dates. The Landsat-8 Operational Land Imager (OLI) and thermal Infrared Sensor (TIRS) satellite image of 19th March 2024 was downloaded from Earth Explorer. Multiple Sentinel-2 datasets over 2 years (23/06/2023 to 12/06/2025) were downloaded from the Copernicus browser. Cloud cover is the main challenge in obtaining cloud-free data sets. All data sets were referenced to the Universal Transverse Mercator (UTM) coordinate system within the grid zone of 55 South. An Area of Interest (AOI) layer was created carefully to extract all these satellite images. The minimum maximum (Min-max) radiometric stretching was performed on all the cropped images for better interpretation and further processing.

TVDI and VHI are the two mathematical models utilized to estimate the health conditions of the oil palm plantation area. Both the drought and health conditions are calculated based on NDVI and LST. Stressed vegetation reflects roughly 30% in the red (R) band and 40% in the near-infrared (NIR), while healthy vegetation reflects 8–10% in the R band and 50–60% in the NIR band. Water stress caused this sudden drop in reflectance in the NIR band. NDVI is an important index calculated by band ratioing between the R and NIR bands. It can easily identify the level of greenness and plant health [23]. The LST identifies the heat level on the topsoil surface [24]. This parameter is derived through the modeling of the 10th band. Total of six steps are followed to derive NDVI and LST from OLI and TIRS bands, namely (1) the calculation of the spectral radiance, (2) the extraction of brightness temperature, (3) the generation of NDVI, (4) determination of vegetation proportion, (5) calculating emissivity of the land surface, and (6) the final extraction of the land surface temperature. The agricultural drought index TVDI is calculated after combining the two most common factors, LST and NDVI [25]. TVDI assesses the drought condition locally, along with wet-edge and dry-edge functions.

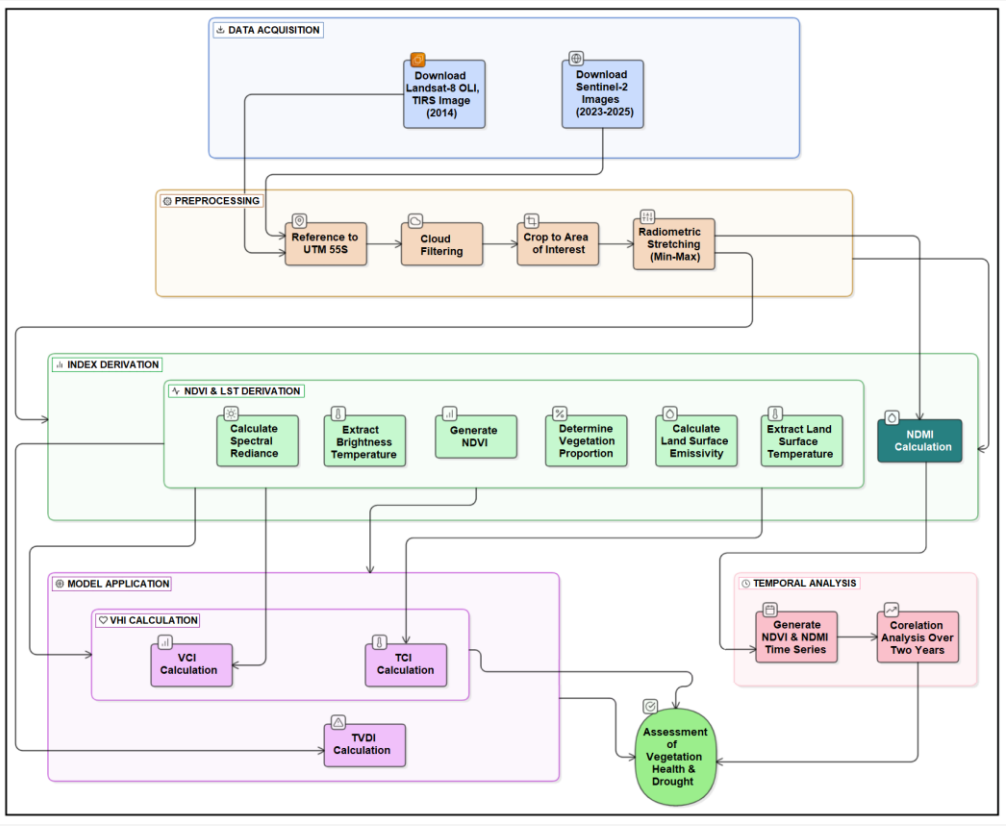

Figure 2: Remote sensing workflow of health and drought analysis over an oil palm plantation

The VHI model, which integrates the VCI and TCI indices, is used to compute the agricultural drought index [26]. Though they use separate observation inputs, both the TCI and VCI indices are calculated using the multispectral bands of Landsat 8 satellite data. The VCI is derived from the NDVI [20] and LST from thermal bands [15]. Another index, the Normalised Difference Moisture Index (NDMI), was used to compute vegetation water content. NDMI was extracted from NIR and Short-wave Infrared (SWIR) bands based on a simple band ratio function. Finally, the Sentinel-2 satellite images were analyzed over two years to understand the temporal correlation between the moisture and the vegetation index. The NDMI and NDVI indices over two years were generated from Sentinel-2 satellite images to measure their temporal correlation. The step-by-step workflow is presented for monitoring the health and drought condition of the oil palm plantation (Figure 2).

5. Results and Discussion

The derived NDVI values ranged from -0.079 to 0.639. The negative value refers to the lower reflected value in the R band and is comparatively higher in the NIR band. The scenario of a positive NDVI value describes a higher reflected value in the R band than in the NIR band. Negative values represent water areas, while positive values represent vegetation characteristics, as presented in Figure 3(a). Higher positive values indicate higher vegetation density and better health conditions. The existing oil palm plantation area displayed a higher NDVI value. The section of the active river channel and the abandoned channel with water are dominated by negative values. As the study area is small, with uniform land use, land cover, and flat topography, the surface temperature is calculated in a narrow range. The calculated LST ranges from 23.291 °C to 29.991 °C. The highest temperatures are observed in the eastern portion and some pockets of the central and northwest portions. In contrast, the lowest temperatures are found in a linear zone from the southeast corner to the southwest and western portions, as shown in Figure 3(b). The dry edge calculation yields LSTmax values ranging from 26.806 to 28.848, while the wet edge equation calculates values from 23.791 to 23.955, respectively. The resulting TVDI ranged from 0.142 to 0.969, as shown in Figure 4(a). A higher value of 1 indicates higher proximity to the drought condition [18]. Resultant VCI ranges from 0 to 99.991.

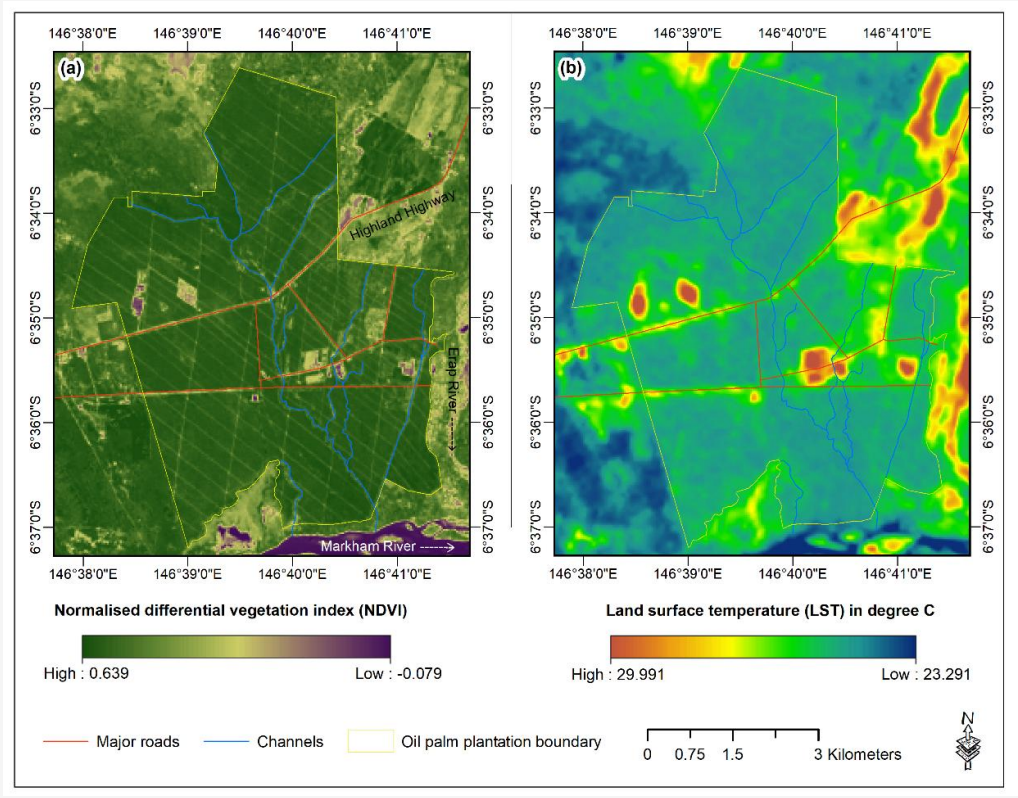

Figure 3: The resulting NDVI and LST: (a) NDVI based on the band ratio of R band and NIR bands, (b) LST based on the 10th band (TIR) of the satellite image

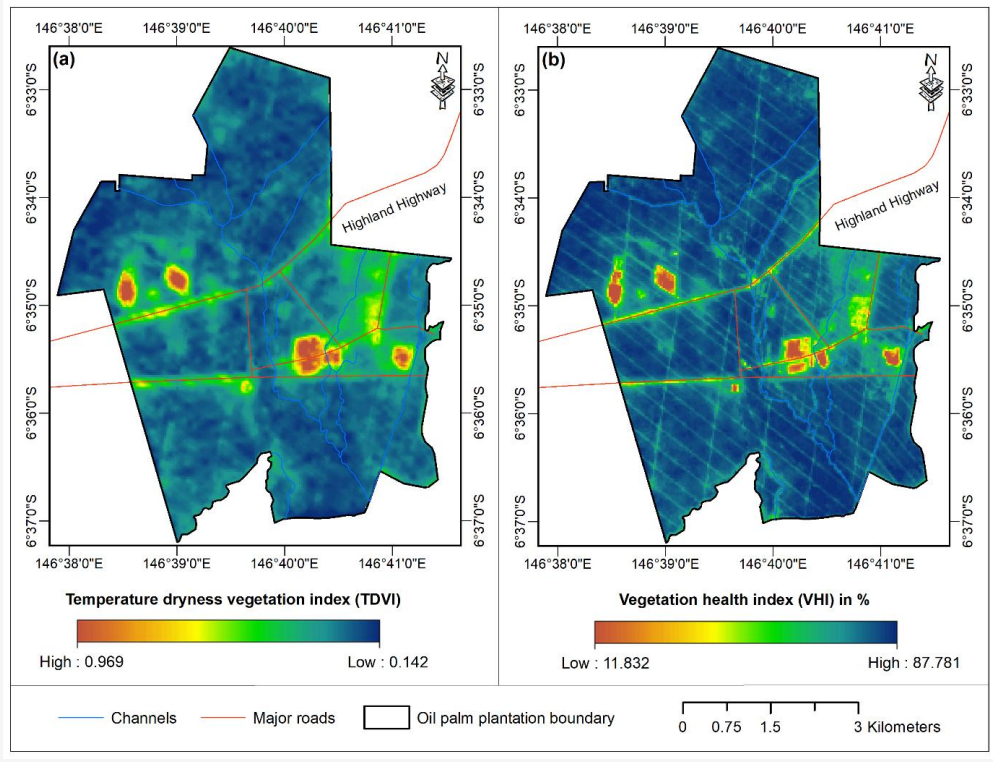

Figure 4: The resulting range output (a) TVDI, and (b) VHI based on NDVI and LST

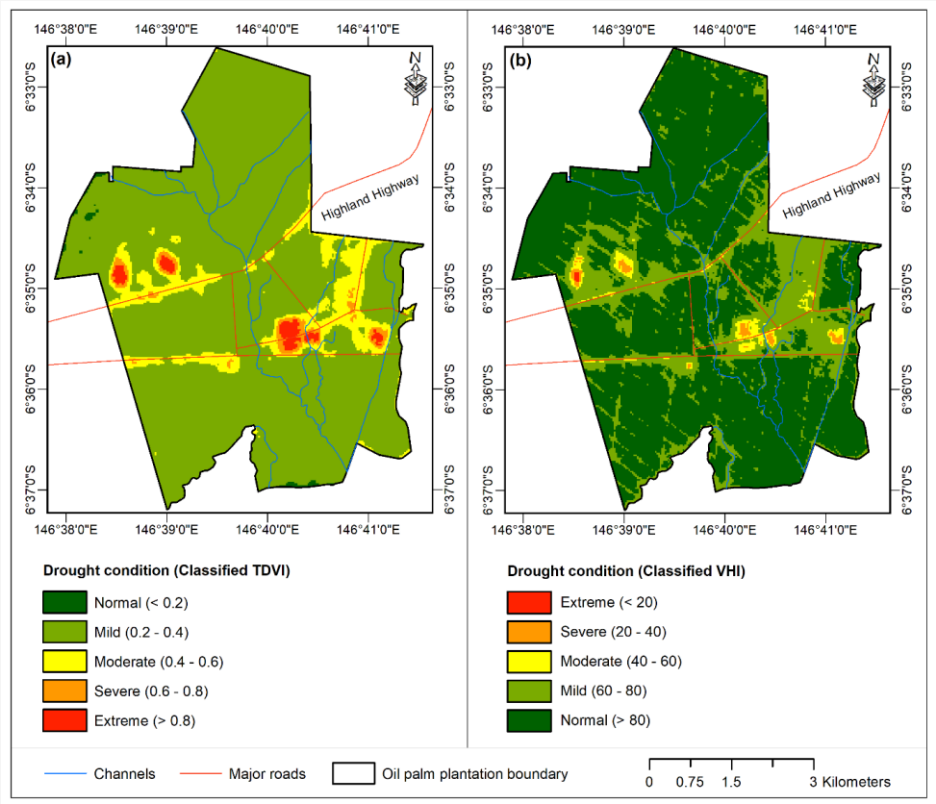

Figure 5: The resulting classified database: (a) TVDI to show agricultural drought conditions, and (b) VHI to express vegetation health conditions

The VHI, a comprehensive technique that combines the TCI and VCI, is used in the study. The VHI may range from 0 to 100. Zero (0) represents extreme dryness, and 100 represents ideal moisture conditions [27]. Figure 4(b) illustrates the resulting VHI output, which ranges from 11.832 to 87.781. A TVDI range value of 0.6 to 0.8 is classified as a 'severe' drought condition, while values exceeding 0.80 are considered 'extreme' drought conditions. The areas experiencing excessive drought conditions are primarily located in the eastern and western parts of the plantation area, where man-made structures and farm buildings are located, as shown in Figure 5(a). Most plantation areas are characterized by normal conditions, except a linear patch in the east and a section in the western part of the plantation, where moderate to severe and even extreme drought conditions are observed. Remnants of old, abandoned channels, featuring stones and gravel, are found in these areas.

The output range of VHI is more than 80, which is classified as a normal condition, and less than 20 as an extreme condition. The significant sections of the plantations are characterized by normal vegetation health, except for a few pockets in the eastern and western parts of the plantation, where vegetation health is mild to moderate, as highlighted in Figure 5(b). These sections are disturbed due to the construction of the access roads to the plantation and other farm infrastructure.

TVDI provides an accurate depiction of the drought situation [28]. TVDI is calculated based on NDVI and LST. The ratio between the R and NIR bands produces the Normalized Difference Vegetation Index (NDVI), which responds dynamically to changes in soil moisture [29]. On the other hand, LST is calculated using NDVI and thermal bands and exhibits a negative correlation with soil moisture levels [30]. The relationship between NDVI and LST for the entire study was moderately negative (R-squared of 0.59), indicating that surface temperature increases as the vegetation index decreases. When calculating wet and dry edge fitting coefficients, the water class with negative NDVI values is ignored. The relationship between NDVI and LST indicates a mild negative correlation for the dry edge, while it is mildly positive for the wet edge. A perfect correlation was observed between LST and TVDI ($R^2 = 0.98$), compared to NDVI and TVDI ($R^2 = 0.48$).

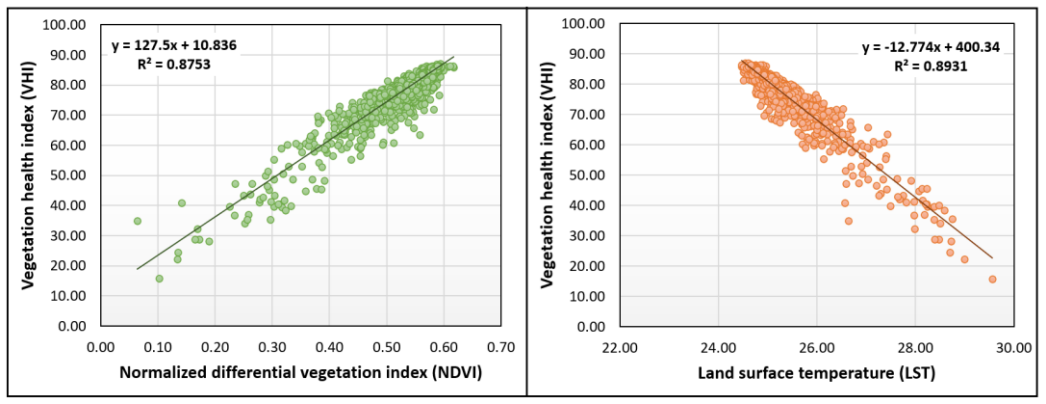

Figure 6: The feature spaces of (a) NDVI and VHI and (b) LST and VHI

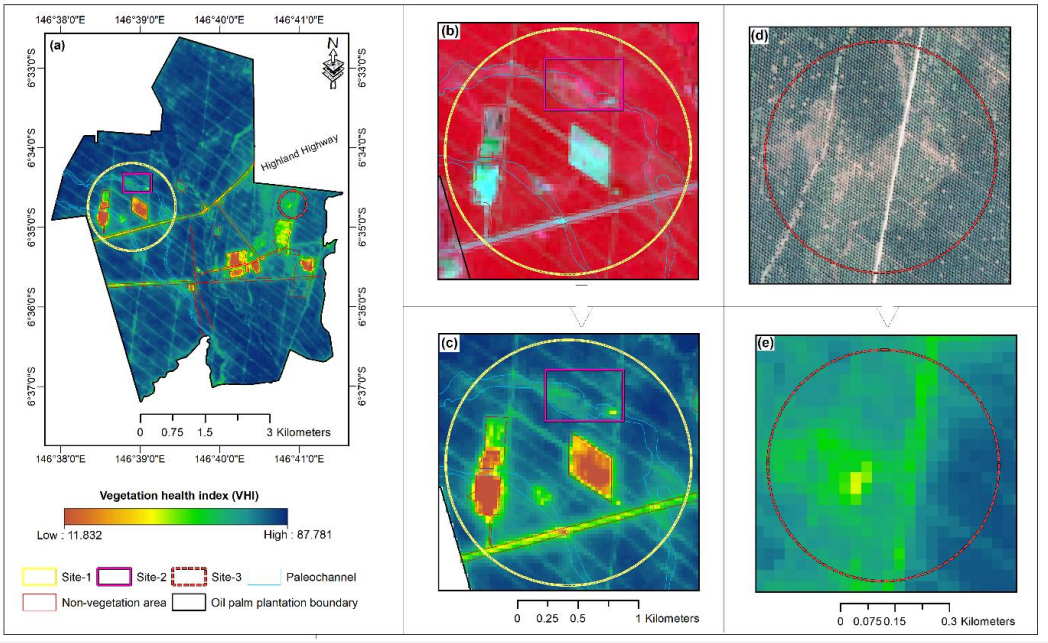

Figure 7: A comparative analysis of: (a) VHI-based results with (b)-(c) Landsat satellite image at site-1 and site-2, and (d)-(e) aerial image at site-3

NDVI is the primary determinant of vegetation health. Figure 6(a) presents a strong coefficient of determination (R-squared of 0.88) between NDVI and VHI. However, a significant negative correlation (R-squared of 0.89) is observed between LST and VHI, as presented in Figure 6(b), suggesting vegetation health declines as surface temperature rises. The resulting VHI is assessed against the actual ground features at the three locations, including farm buildings, access roads within the plantation, and paleochannels, which are highlighted in Figure 7(a), 7(b), 7(c), and 7(d). These evidences prove the quality of the model output generated through VHI analysis from satellite data. The VHI produced more spatial details of drought than the TVDI result. Moderate to severe health issues are emerging in some areas, particularly non-vegetative man-made structures. Remnants of old abandoned channels with stones and gravel, as well as access roads peripheries inside the plantation, characterize the mild health issues in the oil palm plantation. VHI supports monitoring agricultural drought by combining the spatial variation of vegetation and temperature conditions. The resulting VHI was also compared to the Normalized Difference Moisture Index (NDMI) to demonstrate that vegetation health is closely related to the moisture index, as shown in Figures 8(a) and 8(b). The NDMI is typically used to assess the plant's water content and soil moisture levels. The NDMI values range from +1 to -1, with negative values indicating dry soil and positive values indicating wet soil [31].

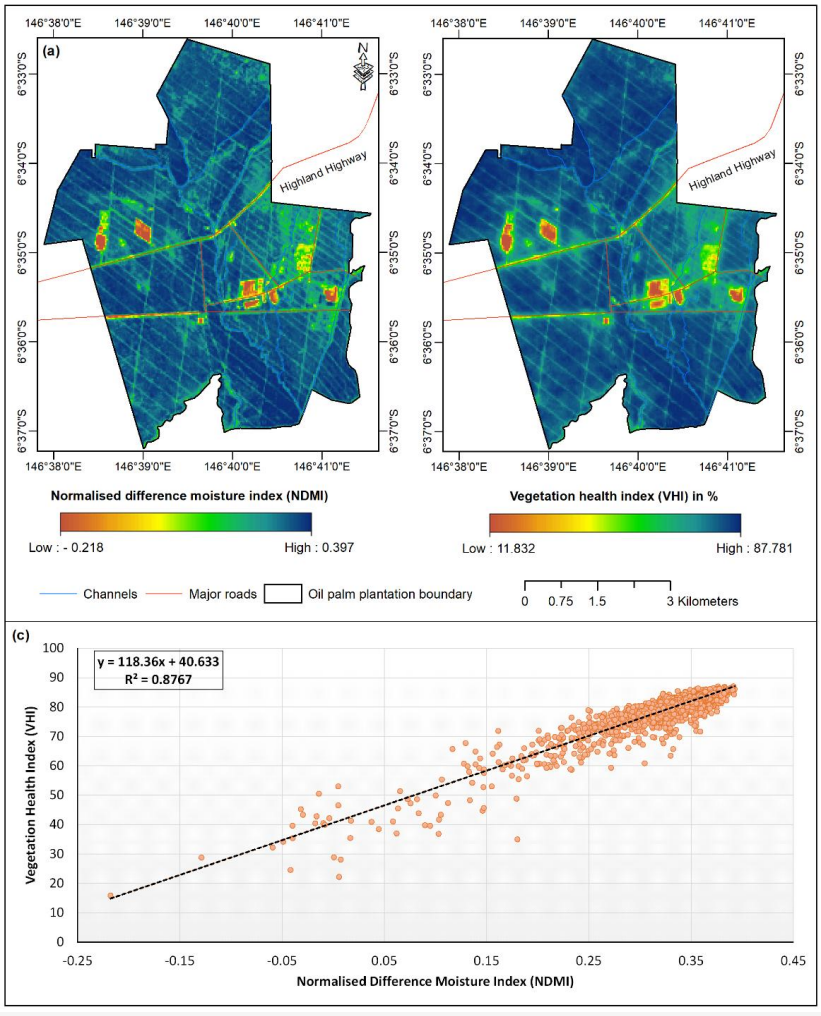

Figure 8: The resulting output (a) NDMI, (b) VHI, and (c) the feature spaces of NDMI and VHI

In this study area, the NDMI ranged from -0.218 to 0.397 (Figure 8(a)). A feature space analysis was conducted between NDMI and VHI. Figure 8(c) highlights that the relationship between NDMI and VHI in the plantation area was highly correlated, with an R-squared of 0.88. This correlation suggests that vegetation health depends on moisture levels in both vegetation and soil. The vegetation health index increases as moisture levels rise and decreases as they fall.

It was found that NDVI is the primary determinant of vegetation health, as indicated by a strong positive coefficient of determination (R-squared of 0.89) between NDVI and VHI. Furthermore, a temporal analysis was performed between NDMI and NDVI to understand how moisture content affects the vegetation index [32]. The Sentinel-2 satellite-driven NDMI and NDVI were compared over 2 years in the plantation site. The result shows that the vegetation index decreases as moisture levels decline (Figure 9(a)). The coefficient of determination between NDMI and NDVI was calculated over 2 years to understand the correlation between moisture levels and the vegetation index. A moderate correlation (R-squared of 0.41) was found between the overall NDVI and NDMI in the plantation area (Figure 9(b)). This correlation is much better than a few other studies, where the correlation between the NDVI and NDMI was calculated as 0.27 [33] and 0.4 [34], respectively. Some inconsistencies were observed while correlating the moisture index and NDVI over the oil palm plantation area [35]. It was also observed that this study derived a better correlation between VHI and LST than some earlier studies [36], which justifies the better outcome of this research. The correlation between VHI and NDVI also improved (0.88) compared to the earlier study in a mixed land use pattern with oil palm-dominated area (0.72) [37].

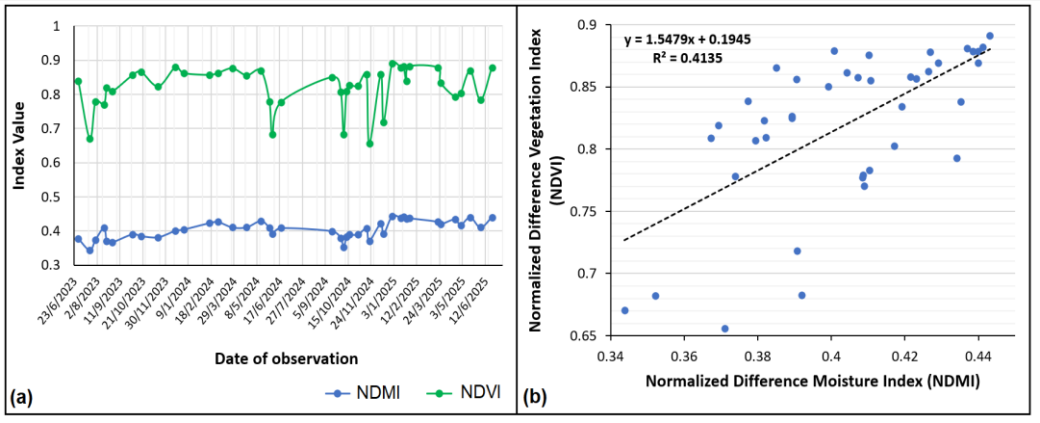

Figure 9: (a) The temporal changes of the NDVI and NDMI, (b) their correlation over 2 years

6. Conclusion

This study emphasizes the advantages of utilizing multispectral satellite data to forecast agricultural health and drought conditions in specific regions by examining temperature and vegetation factors. Estimating and monitoring drought conditions over a large area with a single index may seem overly ambitious and questionable due to varying land use, land cover, climate, and environmental characteristics. The objectives of this study were to analyze the spatial variation of the TVDI and VHI of the plantation area based on satellite-data-driven LST, NDVI, TCI, and VCI; to compare drought patterns based on TVDI and VHI; and to derive the correlation between the moisture and the vegetation index of the plantation area. This research revealed that VHI and TVDI could effectively monitor vegetation health and drought in the Markham Valley region's case study site. The resulting VHI provides more spatial details of drought than the TVDI result. Furthermore, a close and detailed comparative mapping was conducted, where the resulting classes, such as mild, moderate, and severe health issues, were identified in the high-resolution aerial images. These images help to distinguish each tree from the others. The results confirmed that the capabilities of the VHI in identifying spatial differences in vegetation growth and drought conditions are significantly better than those of TVDI. The access roads in the plantation, where no trees are present, were identified as failing by TVDI. The findings indicated that satellite remote sensing technology has a greater impact on monitoring agricultural drought and vegetation health, as measured by TVDI and VHI.

A stronger positive correlation (0.88) was established between NDMI and VHI, suggesting that both indices measure similar drought-related stress on the plantation. The temporal analysis of NDVI and NDMI over two years using Sentinel-2 data indicates a moderate correlation of 0.41, which suggests a connection between plant water content and plant greenness/biomass. However, other underlying factors, like background soil type, surface temperature, and the age of the plantation, also significantly influence these measures, which must be analyzed for better understanding. This research will benefit farm managers in monitoring vegetation health and assessing agricultural drought so that they can adopt different soil conservation methods and irrigation facilities.

Future research should develop an enhanced drought model incorporating high-resolution multispectral satellite data, micro-scale satellite precipitation data, and high-resolution soil moisture data to improve vegetation health and monitor drought. Artificial Intelligence (AI) and Machine Learning (ML) must be used to validate the drought index for the plantation area and link water stress indicators. If high-resolution satellite data is difficult to acquire, an alternative multispectral Unmanned Aerial Vehicle (UAV) is also proposed. Further research also suggested using electrical sensors that can measure the dielectric constant, which is directly related to the water content. This will generate very high-resolution soil moisture data alternatively.

References

[1] Carey, J., (2023). Unearthing the Origins of Agriculture. *Proceedings of the National Academy of Sciences of the United States of America*, Vol. 120(15). https://doi.org/10.1073/pnas.2304407120.

[2] Evans, J. R. and Lawson, T., (2020). From Green to Gold: Agricultural Revolution for Food Security. *Journal of Experimental Botany*, Vol. 71(7), 2211-2215. https://doi.org/10.1093/jxb/eraa110.

[3] Wiset, K., Fisher, R., Baynes, J., Wampe, N., Thom, M., Jackson, W. and Herbohn, J., (2022). What Could Forest Landscape Restoration Look LIKE in the Ramu-Markham Valley of Papua New Guinea?. *Land Use Policy*, Vol. 121. https://doi.org/10.1016/j.landusepol.2022.106322.

[4] Grillakis, M. G., (2019). Increase in Severe and Extreme Soil Moisture Droughts for Europe under Climate Change. *Science of the Total Environment*, Vol. 660, 1245-1255. https://doi.org/10.1016/j.scitotenv.2019.01.001.

[5] West, H., Quinn, N. and Horswell, M., (2019). Remote Sensing for Drought Monitoring & Impact Assessment: Progress, Past Challenges and Future Opportunities. *Remote Sensing of Environment*, Vol. 232. https://doi.org/10.1016/j.rse.2019.111291.

[6] Krueger, E. S., Ochsner, T. E. and Quiring, S. M., (2019). Development and Evaluation of Soil Moisture-Based Indices for Agricultural Drought Monitoring. *Agronomy Journal*, Vol. 111(3), 1392-1406. https://doi.org/10.2134/agronj2018.09.0558.

[7] Wu, B., Ma, Z. and Yan, N., (2020). Agricultural Drought Mitigating Indices Derived from the Changes in Drought Characteristics. *Remote Sensing of Environment,* Vol. 244. https://doi.org/10.1016/j.rse.2020.111813.

[8] Naumann, G., Cammalleri, C., Mentaschi, L. and Feyen, L., (2021). Increased Economic Drought Impacts in Europe with Anthropogenic Warming. *Nature Climate Change*, Vol. 11(6), 485-491. https://doi.org/10.31223/osf.io/fg79t.

[9] Ongsomwang, S. (2025). Responses of Adaptive Capacity to Agricultural Drought Vulnerability and Its Impact, Nakhon Ratchasima, Thailand. *International Journal of Geoinformatics*, Vol. 21(8), 33–52. https://doi.org/10.52939/ijg.v21i8.4363..

[10] Xu, K., Yang, D., Yang, H., Li, Z., Qin, Y. and Shen, Y., (2015). Spatio-temporal Variation of Drought in China during 1961–2012: A Climatic Perspective. *Journal of Hydrology,* Vol. 526, 253-264. https://doi.org/10.1016/j.jhydrol.2014.09.047.

[11] Rimkus, E., Stonevicius, E., Kilpys, J., Maciulyte, V. and Valiukas, D., (2017). Drought Identification in the Eastern Baltic Region Using NDVI. *Earth System Dynamics*, Vol. 8(3), 627-637. https://doi.org/10.5194/esd-8-627-2017.

[12] Kikon, A. and Deka, P. C., (2022). Artificial Intelligence Application in Drought Assessment, Monitoring and Forecasting: A Review. *Stochastic Environmental Research and Risk Assessment*, Vol. 36(5), 1197-1214. https://doi.org/10.1007/s00477-021-02129-3.

[13] Alahacoon, N. and Edirisinghe, M., (2022). Novel Index for Hydrological Drought Monitoring Using Remote Sensing Approach: Standardized Water Surface Index (SWSI). *Remote Sensing*, Vol. 14(21). https://doi.org/10.3390/rs14215324.

[14] Zhang, L., Jiao, W., Zhang, H., Huang, C. and Tong, Q., (2017). Studying Drought Phenomena in the Continental United States in 2011 and 2012 Using Various Drought Indices. *Remote Sensing of Environment*, Vol. 190, 96-106. https://doi.org/10.1016/j.rse.2016.12.010.

[15] Sun, W., Wang, P. X., Zhang, S. Y., Zhu, D. H., Liu, J. M., Chen, J. H. and Yang, H. S., (2008). Using the Vegetation Temperature Condition Index for Time Series Drought Occurrence Monitoring in the Guanzhong Plain, PR China. *International Journal of Remote Sensing*, Vol. 29(17-18), 5133-5144. https://doi.org/10.1080/01431160802036557.

[16] Ezenwaji, E., Nzoiwu, C. and Chima, G., (2017). Analysis of Precipitation Concentration Index (PCI) for Awka Urban Area, Nigeria. *Hydrology: Current Research*, Vol. 8(4), 1-6. https://doi.org/10.1007/s00704-022-04077-6.

[17] Hwang, T. H., Kim, B. S., Kim, H. S. and Seoh, B. H., (2006). The Estimation of Soil Moisture Index by SWAT Model and Drought Monitoring. *KSCE Journal of Civil and Environmental Engineering Research*, Vol. 26(4B), 345-354. https://doi.org/10.12652/Ksce.2006.26.4B.345.

[18] Chen, S., Wen, Z., Jiang, H., Zhao, Q., Zhang, X. and Chen, Y., (2015). Temperature Vegetation Dryness Index Estimation of Soil Moisture Under Different Tree Species. *Sustainability*, Vol. 7(9), 11401-11417. https://doi.org/10.3390/su70911401.

[19] Guo, Y., Han, L., Zhang, D., Sun, G., Fan, J. and Ren, X., (2023). The Factors Affecting the Quality of the Temperature Vegetation Dryness Index (TVDI) and the Spatial-Temporal Variations in Drought from 2011 to 2020 in Regions Affected by Climate Change. *Sustainability*, Vol. 15(14). https://doi.org/10.3390/su151411350.

[20] Domenikiotis, C., Spiliotopoulos, M., Tsiros, E. and Dalezios, N. R., (2004). Early Cotton Yield Assessment by the use of the NOAA/AVHRR Derived Vegetation Condition Index (VCI) in Greece. *International Journal of Remote Sensing*, Vol. 25(14), 2807-2819. https://doi.org/10.1080/01431160310001632729.

[21] Karnieli, A., Bayasgalan, M., Bayarjargal, Y., Agam, N., Khudulmur, S. and Tucker, C. J., (2006). Comments on the use of the Vegetation Health Index Over Mongolia. *International Journal of Remote Sensing*, Vol. 27(10), 2017-2024. https://doi.org/10.1080/01431160500121727.

[22] Li, C., Adu, B., Wu, J., Qin, G., Li, H. and Han, Y., (2022). Spatial and Temporal Variations of Drought in Sichuan Province from 2001 to 2020 Based on Modified Temperature Vegetation Dryness Index (TVDI). *Ecological Indicators*, Vol. 139. https://doi.org/10.1016/j.ecolind.2022.108883.

[23] Bhandari, A. K., Kumar, A. and Singh, G. K., (2012). Feature Extraction using Normalized Difference Vegetation Index (NDVI): A Case Study of Jabalpur City. *Procedia Technology*, Vol. 6, 612-621. https://doi.org/10.1016/j.protcy.2012.10.074.

[24] Thammaboribal, P., Triapthti, N., and Lipiloet, S. (2025). Comparative Analysis of Land Surface Temperature (LST) Retrieved from Landsat Level 1 and Level 2 Data: A Case Study in Pathumthani Province, Thailand. *International Journal of Geoinformatics*, Vol. 21(4), 160–177. https://doi.org/10.52939/ijg.v21i4.4089.

[25] Sandholt, I., Rasmussen, K. and Andersen, J., A., (2002). Simple Interpretation of the Surface Temperature/Vegetation Index Space for Assessment of Surface Moisture Status. *Remote Sensing of Environment*, Vol. 79(2-3), 213-224. https://doi.org/10.1016/S0034-4257(01)00274-7.

[26] Jiang, R., Liang, J., Zhao, Y., Wang, H., Xie, J., Lu, X. and Li, F., (2021). Assessment of Vegetation Growth and Drought Conditions Using Satellite-Based Vegetation Health Indices in Jing-Jin-Ji Region of China. *Scientific Reports*, Vol. 11(1). https://doi.org/10.1038/s41598-021-93328-z.

[27] Erfanian, M., Vafaei, N. and Rezaeianzadeh, M., (2014). A New Method for Drought Risk Assessment by Integrating the TRMM Monthly Rainfall Data and the Terra/MODIS NDVI Data in Fars Province, Iran. *Physical Geography Research*, Vol. 46(1), 93-108. https://doi.org/10.22059/jphgr.2014.50621.

[28] Shi, S., Yao, F., Zhang, J. and Yang, S., (2020). Evaluation of Temperature Vegetation Dryness Index on Drought Monitoring Over Eurasia. *IEEE Access*, Vol. 8, 30050-30059. https://doi.org/10.10.1109/ACCESS.2020.2972271.

[29] Ahmed, A., Zhang, Y. and Nichols, S., (2011). Review and Evaluation of Remote Sensing Methods for Soil-Moisture Estimation. *SPIE Reviews*, Vol. 2(1). https://doi.org/10.1117/1.3534910.

[30] Ghahremanloo, M., Mobasheri, M. R. and Amani, M., (2010). Soil Moisture Estimation Using Land Surface Temperature and Soil Temperature at 5 cm Depth. *International Journal of Remote Sensing*, Vol. 40(1), 104-117. https://doi.org/10.1080/01431161.2018.1501167.

[31] Dhaloiya, A., Denis, D. M., Duhan, D., Kumar, R., Singh, M. C. and Malik, A., (2023). Monitoring Vegetation Health, Water Stress, and Temperature Variation through Various Indices Using Landsat 8 Data. *Indian Journal of Ecology*, Vol. 50(3), 802-810. http://dx.doi.org/10.55362/IJE/2023/3973.

[32] Strashok, O., Ziemiańska, M. and Strashok, V., (2022). Evaluation and Correlation of Sentinel-2 NDVI and NDMI in Kyiv (2017–2021). *Journal of Ecological Engineering*, Vol. 23(9). http://dx.doi.org/10.12911/22998993/151884.

[33] Atefi, M. R. and Miura, H., (2022). Detection of Flash Flood Inundated Areas Using Relative Difference in NDVI from Sentinel-2 Images: A Case Study of the August 2020 Event in Charikar, Afghanistan. *Remote Sensing*, Vol. 14(15). https://doi.org/10.3390/rs14153647.

[34] Song, Y., Xu, H., Liu, T., Xu, J. and Song, X., (2025). Linking Spatiotemporal Variations in Urban Land Surface Temperature to Land Use and Land Cover: A Case Study in Hangzhou City, China. *Ecological Indicators*, Vol. 173. https://doi.org/10.1016/j.ecolind.2025.113336.

[35] Ismail, S. I., Ya'acob, N. S., Kassim, M. and Dzulkefli, N. N., (2025). Seasonal Monitoring and Analysis of Soil Moisture and Vegetation Health in Oil Palm Plantations Using Remote Sensing. *International Journal of Geoinformatics*, Vol. 21(4), 82-96. https://doi.org/10.52939/ijg.v21i4.4069.

[36] Shahzaman, M., Zhu, W., Bilal, M., Habtemicheal, B. A., Mustafa, F., Arshad, M., Ullah, I., Ishfaq, S. and Iqbal, R., (2021). Remote Sensing Indices for Spatial Monitoring of Agricultural Drought in South Asian Countries. *Remote Sensing*, Vol. 13(11). https://doi.org/10.3390/rs13112059.

[37] Samanta, S., (2024). Identification of Agricultural Drought through Vegetation Health Analysis at Erap Station under the Markham Valley of Papua New Guinea. *International Journal of Geoinformatics*, Vol. 20(11), 106-115. https://doi.org/10.52939/ijg.v20i11.3691.